



SA-761079-123401

FORMERLY WILLOW RUN LABORATORIES, THE UNIVERSITY OF MICHIGAN

SIGNAL PROCESSING AND ANALYSIS
DEPARTMENT18 October 1976
Revised 9 November 1976

MEMORANDUM TO: VLA File
FROM: C. C. Aleksoff
SUBJECT: Output Calibration Correction for
Phase Errors

In this memo we investigate calibration correction to the spread function errors calculated in a previous memo¹.

Recall that the spread function is denoted by

$$S(\phi) = S(\phi; x, y) = \int_{uv} \{Ae^{i\phi}\} \quad (1)$$

where $\phi = \phi(u, v)$ is the input phase error and $A = A(u, v)$ is the aperture function. The ideal spread function is $S(0)$. The output error function of interest is given by

$$\bar{\epsilon}_r = 10 \log_{10} |\operatorname{Re} S(\phi) - S(0)| \quad (2)$$

The calibration procedures that can easily be performed at the output plane include:

(a) magnitude scaling by the factor M , i.e.,

1. C. C. Aleksoff, "Phase Error Plots," ERIM memo to VLA File, 16 August 1976, SA-761060-123401.

$$S(\phi) \rightarrow S'(\phi) = \dot{M}S(\phi) \quad (3)$$

(b) Translation by the factors x_0, y_0 , i.e.,

$$S(\phi; x, y) \rightarrow S'(\phi; x, y) = S(\phi; x - x_0, y - y_0) \quad (4)$$

which can be implemented in the input signal by letting

$$\phi \rightarrow \phi' = \phi + \frac{2\pi x_0 u}{\lambda F} + \frac{2\pi y_0 v}{\lambda F} \quad (5)$$

for isoplanetic systems.

(c) Scaling by the factors (a,b), i.e.,

$$x \rightarrow x' = ax, y \rightarrow y' = by \quad (6)$$

(d) Refocusing by a factor c, i.e.,

$$\phi \rightarrow \phi' = \phi + k \sqrt{u^2 + v^2 + c^2} \quad (7)$$



In this memo we will only investigate cases (a) and (b) for one-dimensional errors. That is, we will be calculating equations of the form

$$\bar{\epsilon} = 10 \cdot \log_{10} |\operatorname{Re} MS(\phi - \omega u) - S(0)| \quad (8)$$

where

$$\phi = \frac{2\pi}{\lambda} h \left(\frac{u}{W/2} \right)^n \quad (9)$$

and W is the aperture extent. Recall that

$$A = \frac{1}{W} \operatorname{rect} \left(\frac{u}{W} \right) \cdot T(u) \quad (10)$$

where $T(u)$ is the taper function.

Typical spread function (SF) errors are shown in Figures 1 and 2.

In Figure 1:

For all the curves the phase error is given by

$$\phi = .05 \left(\frac{u}{W/2} \right)^3 \quad (11)$$

i.e., tenth-wave cubic phase error.

The curves are:

- 0) The spread function itself for $T(u) = 1$.
- A) The uncalibrated curve (same as plot 30 in ref. 1) for $T(u) = 1$.
- B) The calibrated curve for $T(u) = 1$. The magnitude scaling was such as to give a null at the center of the SF error curve after translation. i.e., we used

$$\phi = .05 \left[\left(\frac{u}{W/2} \right)^3 - \alpha \frac{u}{W/2} \right] \quad \alpha = 0.6$$

$$M = 1/S(\phi; 0, 0)$$

- C) Same as case B except that $\alpha = 0.2$ and that the Gaussian taper

$$T(u) = \exp \left[\left(\frac{u}{W/2} \right)^2 \ln (.017) \right]$$

was used which corresponds to tapers used by NRAO.

In Figure 2:

The curves are labeled for Figure 1 and the only difference is that fourth order phase error was used, i.e., replace eq. (11) by

$$\phi = .05 \left(\frac{u}{W/2} \right)^4$$



Note that for even order phase errors that the calculation does not need to include translation since the SF is even and real.

Figure 3 is included to show the Gaussian taper (window) used in the calculations and the corresponding spread function. It is seen that the spread function is over three times wider than for no taper.

Figures 4 and 5 show a compilation of maximum spread-function errors extracted from a large set of curves of the type illustrated in Figures 1 and 2. The curves in Figure 4 give the maximum spread-function error as a function of peak-to-peak phase error for various phase error orders. Calibrated and uncalibrated results are given for Gaussian tapered inputs (as shown in Figure 3), as well as for no tapering. Also, the magnitude error for the second order has been included as well as the real part. The curves are for the real part unless otherwise labeled.

Figure 5 also shows the peak spread-function error but where the central part of the error has been excluded, as indicated in the legend. For example, curves B and E exclude the distance from the main lobe to the center of the first side lobe (i.e., the central ± 1.5 X-units in Figures 1 and 2), while curves C and F exclude the entire main lobe and first side lobe (i.e., the central ± 2 X-units in Figures 1 and 2). For a .017 Gaussian tapered input, the exclusion of the main lobe and first side lobe (i.e., the central ± 4 X-units in Figures 1, 2, and 3) gives curve H.

It is immediately obvious that the curves tend to be straight lines for these small phase-error plots. The odd orders go as the square of the phase error and the even



orders in proportion to the error (see Appendix A). The odd orders are more troublesome. The calibration procedure improves the results. Exclusion of the main lobe region for determining the maximum spread-function error gives a very significant improvement. For example, considering the third order, the 1% criteria indicates $\lambda/71$ phase error allowance for no taper, no calibration, and no exclusion but a $\lambda/10$ phase error is allowed if both calibration and exclusion are used (and no taper). If the .017 Gaussian taper is also allowed, then the improvement is extremely large. We should also note that taking the real part also gives a large improvement for the even-order phase errors.

CCA/pw

cc: I. Cindrich
J. Fienup
M. Hidayet
A. Klooster

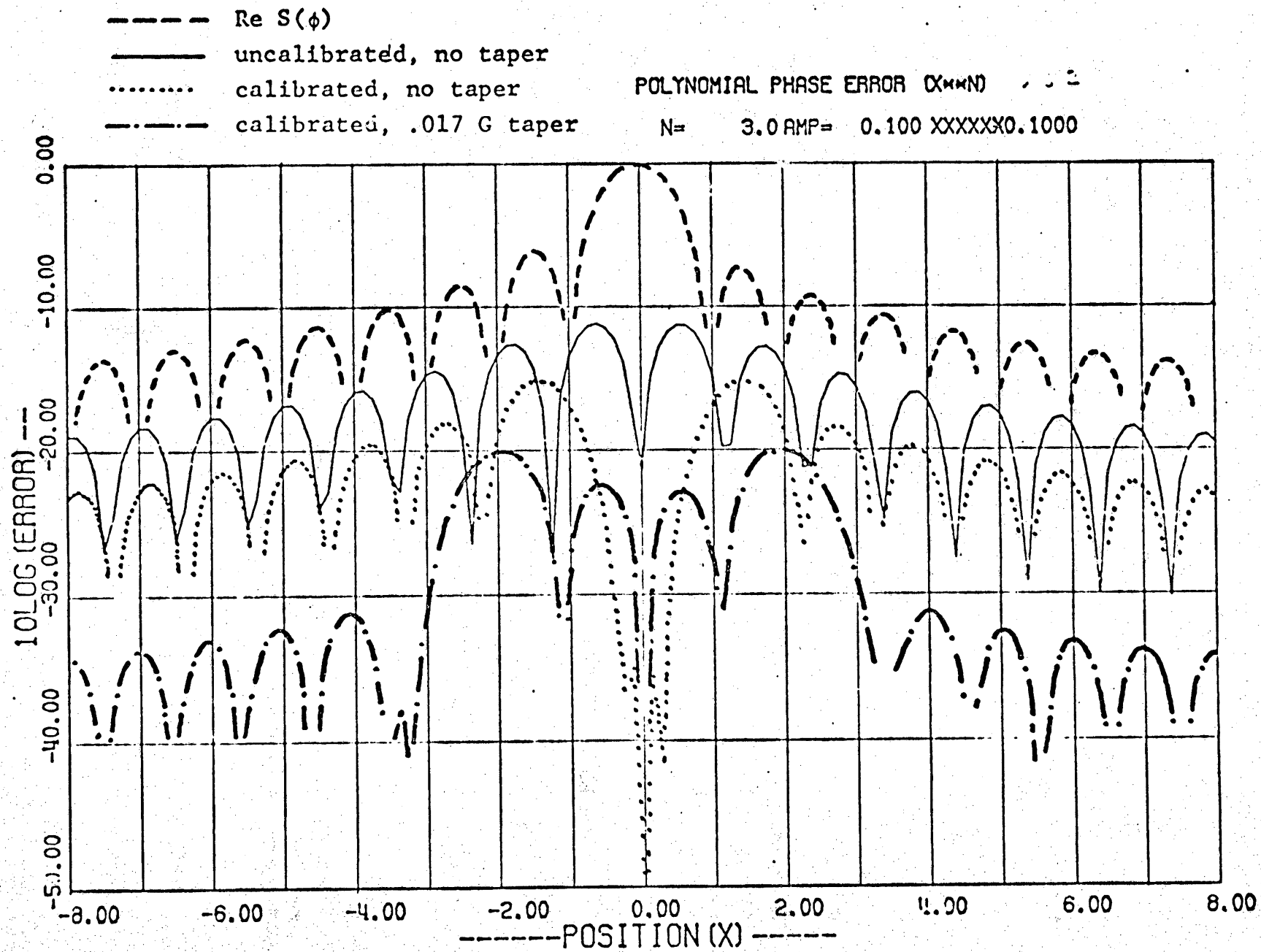


FIGURE 1

- A uncalibrated, no taper
- B ————— calibrated, no taper
- C - - - - - calibrated, .017 G taper

POLYNOMIAL PHASE ERROR (X**N)

N= 4.0 AMP= .1000 XXXXXX0.0000

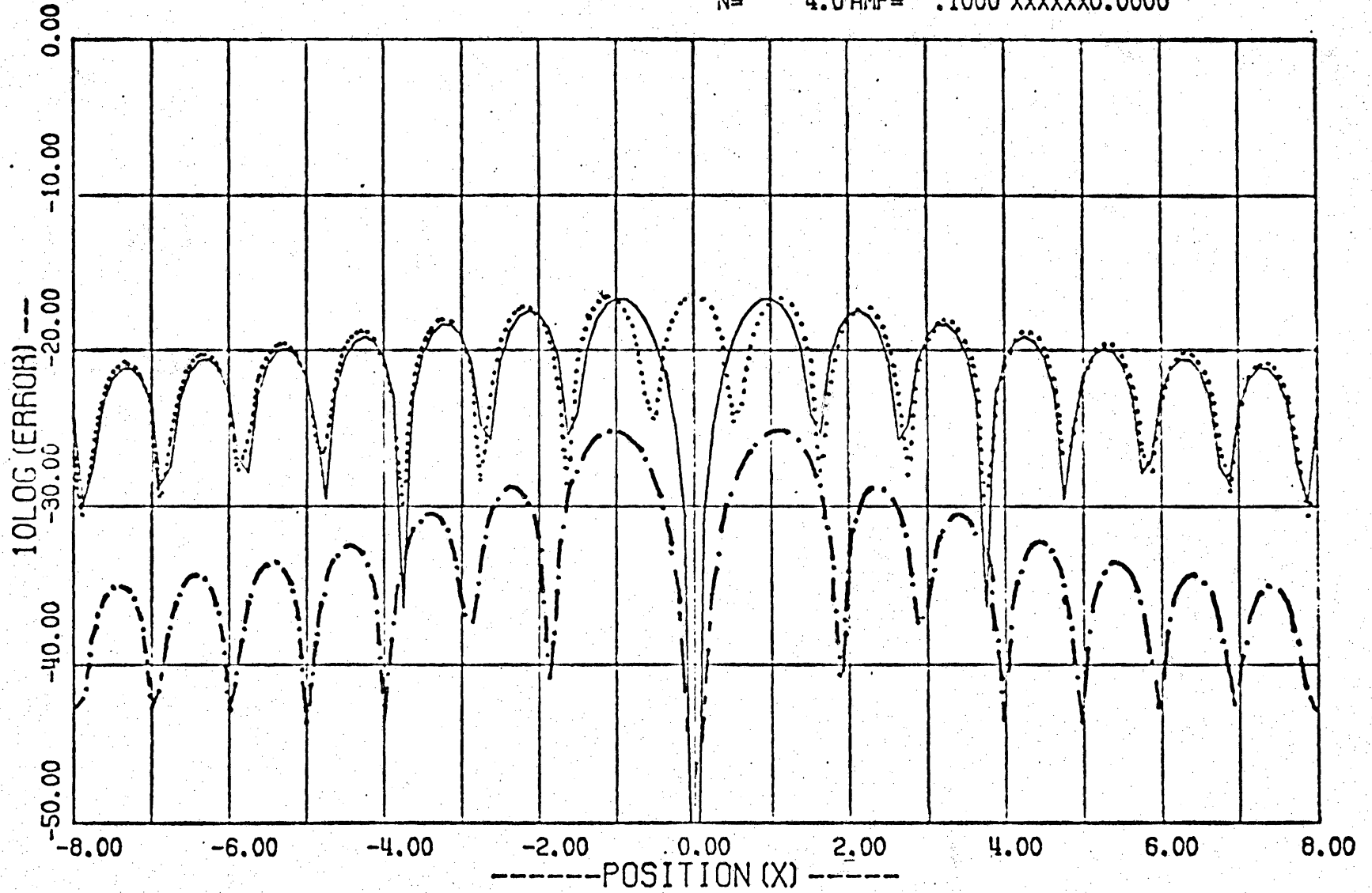


FIGURE 2

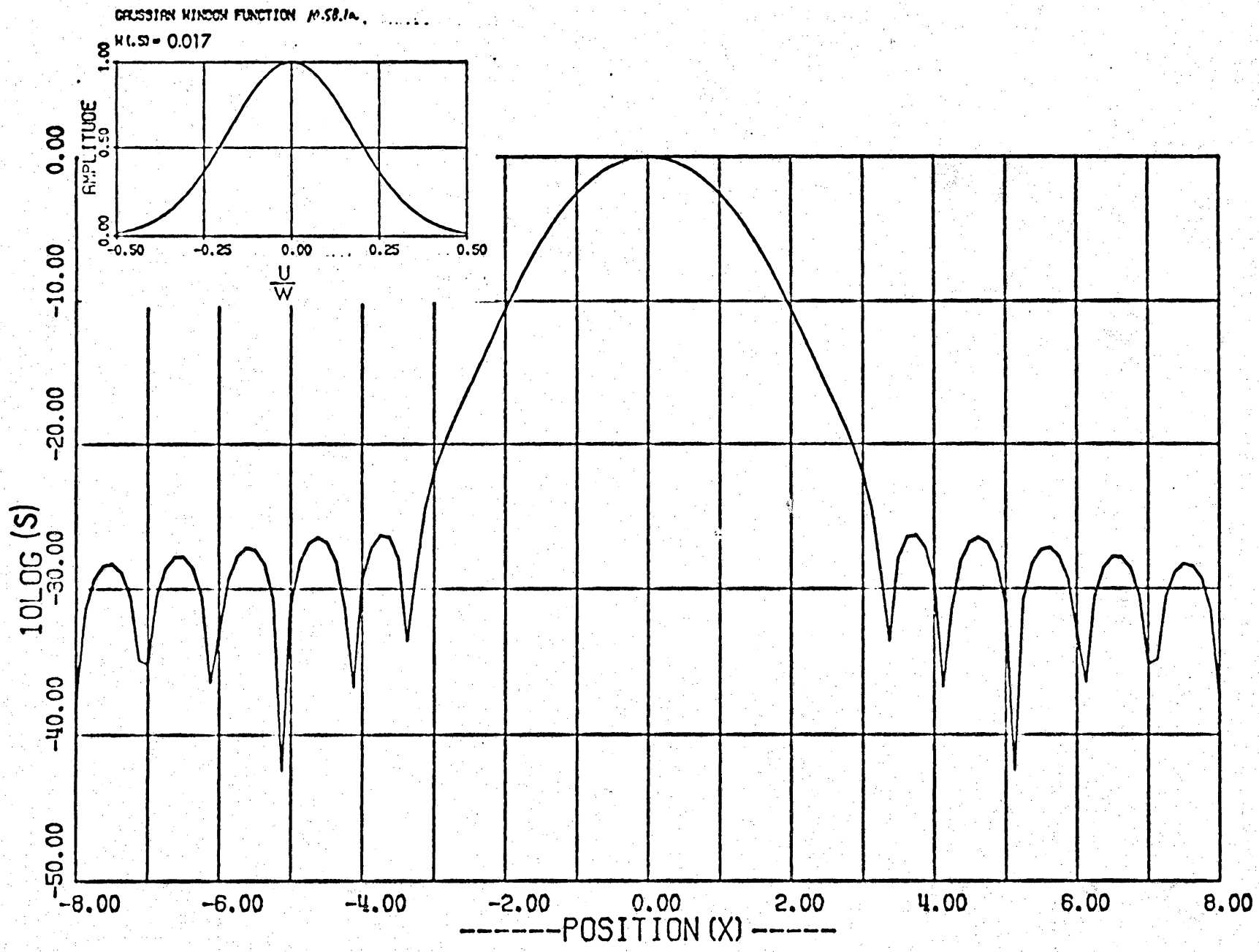


FIGURE 3

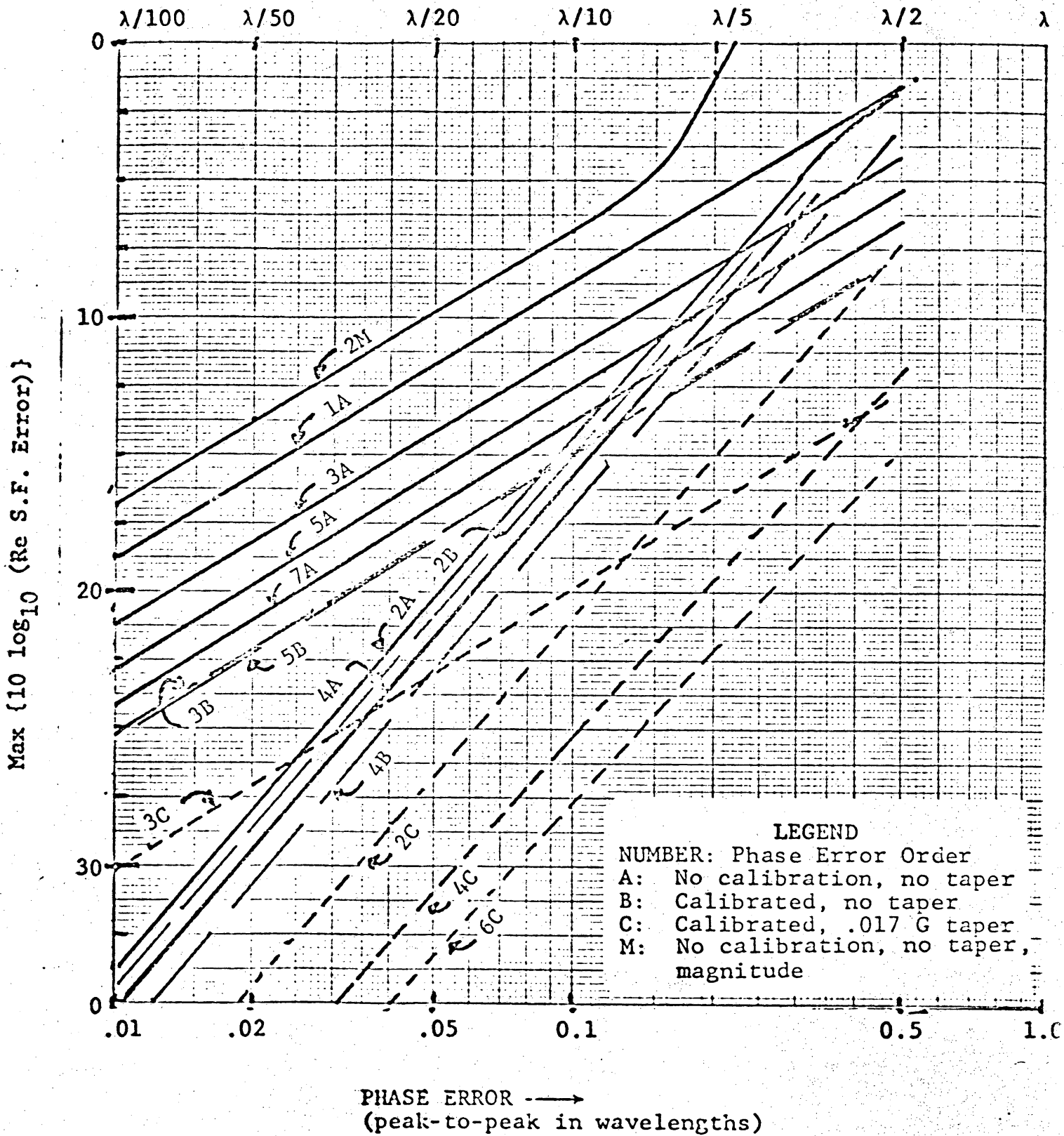
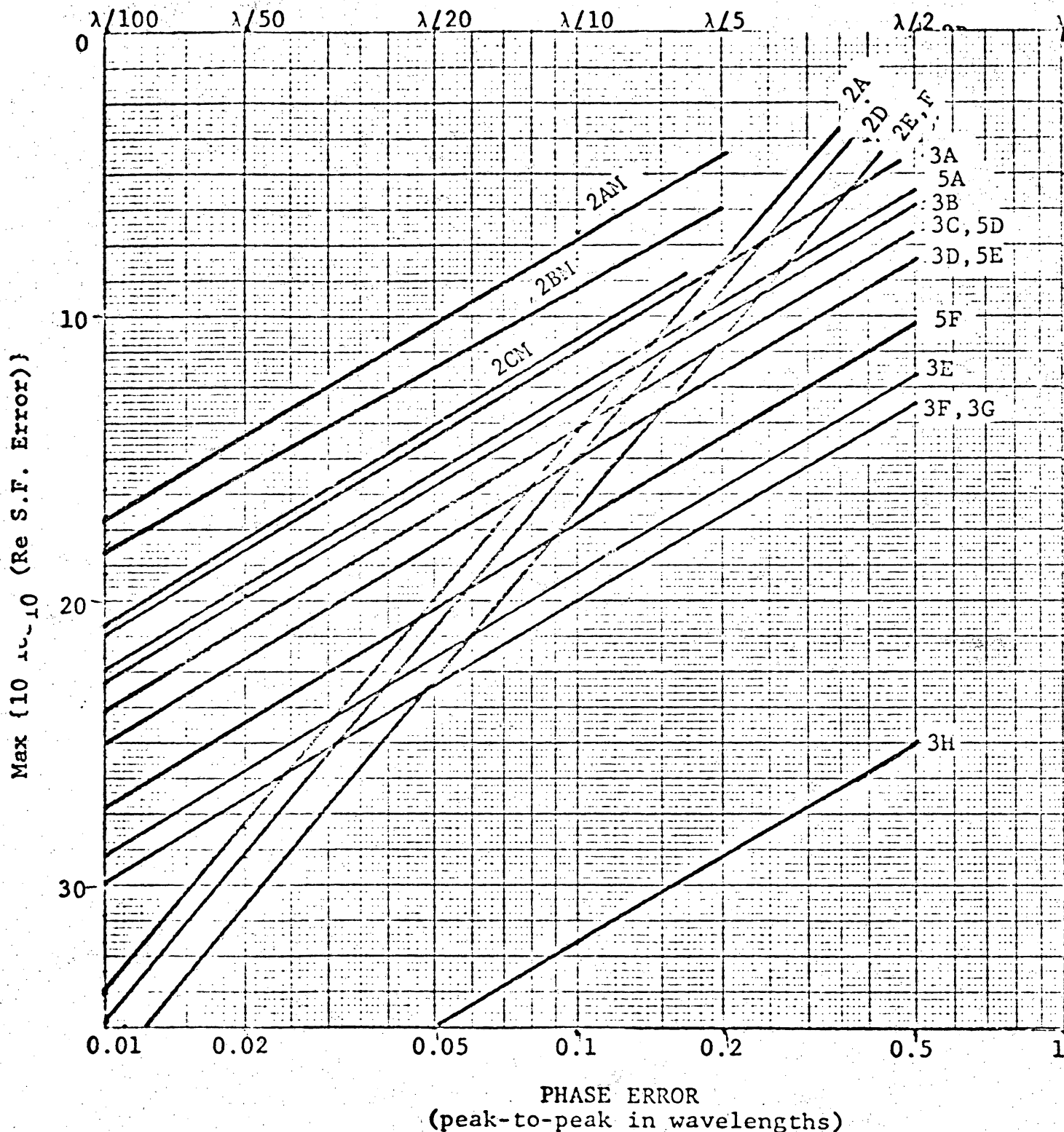


FIGURE 4



LEGEND

NUMBER: Phase Order

- A: No Calibration, no taper, no exclusion
- B: No calibration, no taper, +1.5 X-units excluded
- C: No calibration, no taper, +2.0 X-units excluded
- D: Calibrated, no taper, no exclusion
- E: Calibrated, no taper, +1.5 X-units excluded
- F: Calibrated, no taper, +2.0 X-units excluded
- G: Calibrated, .017 G. taper, no exclusion
- H: Calibrated, .017 G. taper, +4 X-units excluded
- M: Magnitude (Real Part Otherwise)

FIGURE 5

Appendix A

ANALYSIS OF OUTPUT ERRORS DUE TO
SMALL INPUT PHASE ERRORS

The spread-function errors (S.F. errors) shown in this memorandum, which have been numerically computed using FFT's, all tend to be straight lines for phase errors of less than $\lambda/2$. This implies that retaining only the first few terms of a power series expansion of the exponential term is sufficient in analyzing the results. This expansion is used below to describe the results obtained in this memorandum.

BASICS

Consider the output error given by

$$\Delta B = B(\phi) - B(0) \quad (\text{A-1})$$

where $B(\phi) = B(\phi; x, y)$ is the output brightness with phase error $\phi = \phi(u, v; x, y)$ and $B(0)$ is the ideal brightness. The brightness is given by

$$B(\phi) = \mathfrak{F} \left\{ VA e^{i\phi} \right\} \quad (\text{A-2})$$

where $V = V(u, v)$ is the visibility and $A = A(u, v)$ is the aperture description.

We now assume that $\phi \ll 1$ such that the expansion

$$e^{i\phi} = 1 + i\phi - \phi^2 \quad (\text{A-3})$$

A-2

is appropriate. Then (A-1) can be written as

$$\Delta B = \mathfrak{F} \left\{ VA(i\phi - \phi^2) \right\} \quad (A-4)$$

We now expand ϕ in the power series

$$\phi = 2\pi \sum_{m,n} c_{mn} u^m v^n \quad (A-5)$$

where the coefficients $c_{mn} = c_{mn}(x, y)$. All summations are assumed to go from 0 to ∞ unless otherwise specified. Then

$$\phi^2 = (2\pi)^2 \sum_{m,n} d_{mn} u^m v^n \quad (A-6)$$

where the coefficients d_{mn} can be written as a combination of c_{mn} coefficients.

Using the well-known relationship for derivatives of a Fourier transform gives

$$\mathfrak{F} \left\{ u^m v^n AV \right\} = \frac{B_{mn}(0)}{(-2\pi i)^{m+n}} \quad (A-7)$$

where

$$B_{mn}(0) = \frac{\partial^m}{\partial x^m} \frac{\partial^n}{\partial z^n} B(0) \quad (A-8)$$

Thus, from (A-4) to (A-7)

$$\Delta B = \sum_{m,n} \frac{2\pi i c_{mn} - 4\pi^2 d_{mn}}{(-2\pi i)^{m+n}} B_{mn}(0) \quad (A-9)$$

which shows that the output error is a sum of derivatives of the ideal response.

A-3

If we are interested in the real part of ΔB where $B_{mn}(0)$ is real due to the fact that VA is hermetian, then

$$\text{Re } \Delta B = \left\{ \begin{array}{l} \sum_{\substack{m, n \\ m+n \text{ odd}}} (-1)^P \frac{c_{mn}}{(2\pi)^{m+n-1}} B_{mn}(0) \\ \text{where } P = \frac{m+n-1}{2} \\ \\ \sum_{\substack{m, n \\ m+n \text{ even}}} (-1)^P \frac{d_{mn}}{(2\pi)^{m+n-2}} B_{mn}(0) \\ \text{where } P = \frac{m+n+2}{2} \end{array} \right.$$

(A-10)

Thus, the even summed terms go directly as the phase error coefficients, while the odd summed terms go as the product of the phase error coefficients.

ONE-DIMENSIONAL EXAMPLE

Let

$$\phi = 2\pi h_m \left(\frac{u}{W/2} \right)^m$$

$$A = \frac{1}{W} \text{rect} \left(\frac{u}{W/2} \right)$$

and $V = 1$.

Then

$$\phi^2 = 4\pi^2 h_m^2 \left(\frac{u}{W/2} \right)^{2m}$$

A-4

and

$$B(0) = \text{sinc}(Wx)$$

Hence,

$$c_{m,0} = \frac{h_m}{(W/2)^m}$$

and

$$d_{2m,0} = \frac{h_m^2}{(W/2)^{2m}}$$

Then (A-9) becomes

$$\begin{aligned} \Delta B &= 2\pi(i)^{m+1} h_m \text{sinc}_m(Wx) \\ &+ 4\pi^2 (-1)^{m+1} h_m^2 \text{sinc}_{2m}(Wx) \end{aligned}$$

where

$$\text{sinc}_m(Wx) = \frac{1}{(\pi W)^m} \frac{\partial^m}{\partial x^m} \frac{\sin(\pi Wx)}{Wx}$$

Thus, if m is even,

$$\text{Re } \Delta B = -4\pi^2 h_m^2 \text{sinc}_{2m}(Wx)$$

and if m is odd (retaining only the lowest order term)

$$\text{Re } \Delta B = 2\pi (-1)^{(m+1)/2} h_m \text{sinc}_m(Wx)$$

A-5

We see that the odd-order terms are proportional to the amplitude h_m , while the even-order terms are proportional to h_m^2 , which was confirmed by the curves formed using the FFT. The shape of the curves are determined by the proper derivative of the sinc function. The effect of taking the real part is to drop the linear term in h_m for the even-order terms.